JOURNAL OF AIRCRAFT
Vol. 35, No. 1, January–February 1998

Numerical Simulations of Commercial Aircraft Wakes Subjected to Airport Surface Weather Conditions

Robert L. Ash*
Old Dominion University, Norfolk, Virginia 23529-0013
and
Z. Charlie Zheng†
University of South Alabama, Mobile, Alabama 36688

Using tower flyby data for validation, we have developed a two-dimensional numerical simulation of the influence of surface weather conditions on wake vortex motion and decay for representative commercial aircraft. Our simulations support the conjecture that the ratio of eddy viscosity to kinematic viscosity, appropriate for modeling aircraft wakes, scales linearly with circulation, which yields a nominally constant equivalent Reynolds number for all commercial aircraft sizes. We have tested the constant eddy viscosity approximation for three different aircraft types and six surface weather states, showing the utility of the approach in predicting wake vortex motion and decay. Subsequently, we have shown how data from one aircraft flight test can be used to infer the decay behavior of another, and we have examined the influence of the six surface weather states on the vortex decay behavior predicted for a large commercial aircraft. Based upon these simulations, we have determined that the two-dimensional, constant eddy viscosity approach can be useful in assessing the influence of surface weather conditions on wake vortex decay.

Introduction

UNANTICIPATED encounters with residual aircraft wake vortices during terminal flight operations are highly undesirable. Not only do they impose severe flight control demands on aircraft that are flying in limited airspace, but the need to avoid such encounters is a primary consideration controlling aircraft spacing specifications around congested airports.[1,2] If the aircraft spacing specifications are too conservative, substantial reductions in passenger throughput result at busy airports. On the other hand, if the spacing standards are overly optimistic, potentially dangerous vortex encounters can occur.[2] The present study was concerned with developing numerical models for the wake vortex behavior of representative commercial aircraft types to better understand how their generated axial vortices behave in response to weather conditions in the lower atmosphere. In that way, different aircraft and surface weather combinations can be investigated systematically to assess the conditions under which wake vortex hazards either persist for longer periods or are dissipated more rapidly.

The initial strengths and locations of the two primary axial vortices produced by a particular airplane in flight can be estimated rather accurately using classical aerodynamic theory.[3] However, prediction of the subsequent motion and decay history of the vortex system requires modeling techniques that include viscous and turbulent effects along with atmospheric wind and temperature distributions.[4] Those considerations are outside of classical aerodynamic theory. Furthermore, when the aircraft is in terminal flight, coupling of the vortex system with the ground must be included, and the classical exclusion of surface viscous effects produces completely different long-term vortex trajectory predictions.

Aircraft wake vortex behavior has been an important safety consideration in air traffic control for some time. Donaldson and Bilanin[5] provided a comprehensive summary of the research prior to 1975, while amore recent overview of current research is contained in the proceedings of the 1991 FAA International Wake Vortex Symposium.[6] Aircraft spacing standards during terminal flight operations are based on rather empirical data. Although anecdotal information implies that surface weather alters wake vortex hazard conditions, there are no allowances for surface weather conditions in the spacing standards, other than the differentiation between instrument and visual flying rules.[1]

Our goal has been to model numerically the wake vortex behavior of different types of commercial aircraft subjected to a range of surface weather conditions. However, rather than using numerical models with restricted Reynolds number limitations, we have exploited the recent study of Zeman,[7] which determined that high Reynolds number turbulent axial vortices are controlled more by localized viscous effects than by turbulent phenomena. In that way, we have been able to develop an equivalent eddy viscosity for a particular aircraft wake vortex system and model subsequently the motion and decay of that system under different types of weather conditions. The constant eddy viscosity model causes the simulated vortex cores to dilate relative to the observed behavior of actual aircraft wake vortices, but our simulations show that the overall rates of decay are consistent with actual flight data. Although the actual upset potential for a small general aviation aircraft resulting from an encounter with the wake of a large commercial aircraft will be underestimated via the present eddy viscosity approximation, we have found that the expanded vortex cores produced by the numerical simulation do not influence appreciably the predicted upsets represented by other commercial aircraft whose wing spans are comparable with the generator aircraft.

Zheng and Ash[8] have discussed the numerical model and its accuracy. The aircraft wake vortex system has been treated as a two-dimensional, unsteady flow using vorticity and stream

Presented as Paper 96-0660 at the AIAA 34th Aerospace Sciences Meeting, Reno, NV, Jan. 15–19, 1996; received March 3, 1997; revision received July 3, 1997; accepted for publication July 3, 1997.

*Professor, Aerospace Engineering Department. Associate Fellow AIAA.

†Assistant Professor, Mechanical Engineering Department. Member AIAA.

function as the dependent variables. The wake vortex pair has been initialized using aircraft weight, wing span, flight speed, and altitude to prescribe a pair of vortices of given strength and location, based upon classical theory.[3] Atmospheric weather effects have been treated as steady-state conditions, with spatial variations occurring only in the vertical direction. The Boussinesq approximations have been used to incorporate temperature and density effects in the equations of motion,[9] but because of the limited vertical region being considered for aircraft vortex flow simulations, it was not necessary to employ the potential temperature.[10]

Turbulence effects in wake vortex core regions represent unusual modeling problems caused by the complex flow physics associated with axial vortices. The very strong centripetal forces that exist along the vortex axes damp out turbulent fluctuations in the central region of the vortex cores, while turbulence in the outer swirling flow regions tends to be more like a passive scalar effect than a directly coupled flow effect. However, in the annular region between the vortex core centers and their outer swirling flows, turbulent fluctuations are believed to be controlling.[11] As characteristic vortex Reynolds numbers are increased, the region over which these turbulent processes are dominant becomes very small in comparison to the region over which the vortex pair is operative. Hence, a very important aspect of aircraft wake vortex flow becomes unresolvable using conventional numerical techniques, even at vortex-based Reynolds numbers that are well below those characterizing commercial aircraft flight conditions. The constant eddy viscosity model smears that turbulence zone deliberately, to represent overall vortex decay correctly. However, the appropriate eddy viscosity level must be calibrated with actual flight data.

The idea of an equivalent eddy viscosity model for turbulent axial vortices is very old. Squire[12] proposed that eddy viscosity should be proportional to circulation in an equivalent laminar vortex model he developed in 1954. That idea was explored subsequently by others.[13–15] Unfortunately, the controlled experiments used in the earlier studies only spanned the circulation-based Reynolds number range $10^3 < \Gamma/\nu < 10^6$, and typical commercial aircraft wake vortices generate Reynolds numbers that are approximately one order of magnitude larger.

Owen[13] and Iverson[15] attempted to correlate flight data, but the available experimental data were either for very small airplanes or their results were inferred indirectly from other flight measurements with uncertain associated errors. Furthermore, the only way the equivalent eddy viscosity could be estimated was by assuming that the shape of the actual wake vortex velocity profile was similar to the profile employed by Squire.[12] In the vicinity of the ground, where the earlier flight measurements were taken, the vortex trajectories were altered and their associated velocity profiles are known to become asymmetric, departing from Squire's model.

To avoid invoking a nonphysical symmetry condition associated with the unknown measurement errors of the earlier flight experiments, we have combined the controlled experimental decay results, compiled by Owen[13] and Lezius[14] at lower Reynolds numbers, with our simulations of data from the more recent commercial aircraft flight experiments conducted by the National Oceanic and Atmospheric Administration (NOAA) at Idaho Falls, Idaho,[16] to develop an eddy viscosity vs circulation correlation. Because the wake vortex experiments conducted at Idaho Falls were measured in ground effect and were subject to local surface weather, which changed with each flight, we have used a single, well-documented vortex decay flight experiment as our calibration case[17] to estimate eddy viscosity for one aircraft at one flight condition. Then, we have extended Squire's constant eddy viscosity model[12] across the commercial aircraft circulation range. Because Squire's assumption of a linear relationship between eddy viscosity and circulation yields a constant equivalent Reynolds number for all commercial aircraft, parametric studies of other flight conditions were justified. Subsequently, we have employed the eddy viscosity correlation to simulate five additional aircraft–weather combinations and compared those simulations with actual flight measurements. Finally, we have discussed how the techniques developed in this study can be generalized to other aircraft/weather combinations and then showed how surface weather influences decay for a large commercial aircraft.

Idaho Falls Data Sets

A total of 241 tower flyby tests were reported in the Idaho Falls test campaign.[16] The flight tests utilized B 757-200, B 727-222, and B 767-200. Many of the tests produced inconclusive or incomplete data, but a wide variety of aircraft/weather combinations were recorded. Working at NASA Langley Research Center, six flight measurements sets were chosen to test our numerical approach. Those measurement flights are summarized in Table 1 and involved all three aircraft types flying in both landing and takeoff configurations in a variety of surface weather conditions. Initial circulation levels were estimated using the aircraft weight and airspeed data tabulated by Garodz and Clawson.[16] Because fuel was being consumed during the flight, the aircraft weights were considered to be nominal estimates. The surface wind and temperature profiles for the six flight tests are displayed in Figs. 1 and 2. The meteorological measurements were made primarily on a 200-ft (61-m) tower, and were combined with weather balloon measurements above that height. Also shown in Figs. 1 and 2 are the polynomial curve fits that were used to represent that corresponding velocity and temperature distribution in the numerical simulations.

Table 1 Summary of tower flyby simulation cases

Aircraft type	Run number (date)	Configuration[a]	Height above ground, ft	Nominal crosswind speed, kn	Bulk Richardson no.	Meteorological state
B 757-200 (calibration)	9 (9/23/90)	L-30-135	230	11	0.5	Stable/moderate shear
B 757-200	30 (9/25/90)	L-25-136	230	8.5	−5.4	Unstable/low shear
B 757-200	45 (9/26/90)	TO-20-142	260	5.5	1.9	Stable/low shear
B 767-200	7 (9/29/90)	L-25-140	230	8	0.6	Stable/moderate shear
B 767-200	23 (9/30/90)	TO-15-140	250	3.5	16	Stable/low shear
B 727-222	22 (9/23/90)	L-30-118	250	9	0.04	Near-neutral/moderate shear

[a]Tests were flown nominally at constant altitude; aircraft were configured either for landing (*L*) or take-off (*TO*). The middle number represents the flap setting in degrees, and the last number is the indicated air speed in knots.

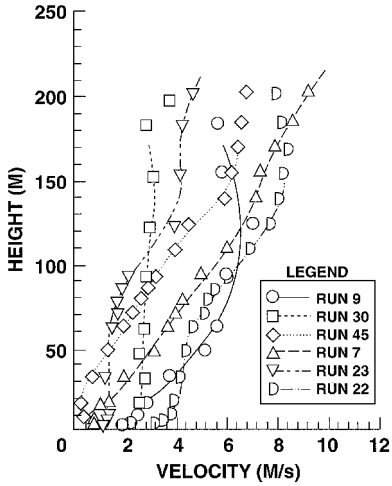

Fig. 1 Measured surface wind velocity profiles for the six Idaho Falls flight tests defined in Table 1. The corresponding curves represent the polynomial data fits used in the numerical simulations.

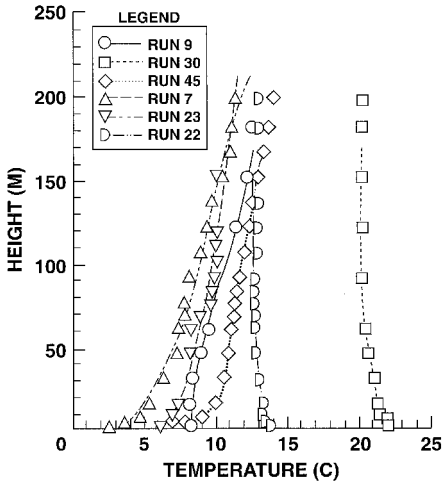

Fig. 2 Measured and fitted surface temperature distributions for the six Idaho Falls flight tests.

Eddy Viscosity Calibration Test

To date, the most thoroughly documented flight measurement case during the Idaho Falls test series has been informally called run 9, as indicated in Table 1. That test[17] utilized a Boeing 757 aircraft, designated UAL-B-757-200, flying in level flight at an altitude of 230 ft (70 m) above the ground, and was used to calibrate our numerical simulations. The airplane was trimmed for landing (flaps deployed at 30 deg), with a nominal gross weight of 192,000 lb (87,000 kg), flying with an airspeed of 135 kn. That condition corresponded to an initial circulation level Γ_∞ of 3900 ft^2/s (365 m^2/s) and a circulation Reynolds number Γ_∞/ν of 2.6×10^7. The surface weather during that flight was classified as stable with a surface air temperature of 47°F (8.6°C) and a nominal crosswind speed of 11.1 kn.

Stratification effects are included in the numerical simulations through the Brünt–Väisällä frequency N, given by

$$N^2 = g \left.\frac{\mathrm{d}\theta}{\mathrm{d}z}\right/ \theta(z) \tag{1}$$

where g is the acceleration of gravity (acting in the z direction), and θ is the potential temperature related to local absolute temperature $T(z)$ and ambient pressure $p(z)$ by

$$\theta(z) = T(z)[p(z)/p(0)]^{(\gamma-1)/\gamma} \tag{2}$$

where γ is the ratio of specific heats. In the cases studied here, $p(z)/p(0) \approx 1$, so that $\theta(z) \approx T(z)$.

If we define an equivalent eddy viscosity-based Reynolds number as

$$R = \Gamma_\infty/\varepsilon \tag{3}$$

where ε is the eddy viscosity, the objective in calibrating our simulation of run 9 was to estimate an ε that best represented the circulation decay measured in the actual flight test.

Circulation histories have been extracted from tower flyby measurements with great difficulty. Because instantaneous weather and the location and symmetry of the primary wake vortices are neither known nor controlled, the velocity histories measured from a finite number of discrete sensor locations must be used to extract and reconstruct the entire wake vortex velocity field in a two-dimensional vertical plane. Typically, symmetry is enforced by combining the measured velocity data from one side of the vortex axis with data from the opposite side, and the ambient winds are assumed either to be constant or to cancel. Then, instantaneous circulation can be inferred by using

$$\Gamma(r) = 2\pi r V_\theta(r) \tag{4}$$

where V_θ is the local tangential velocity component, and r is the radius with respect to the vortex center. However, circulation only asymptotes to $\Gamma_\infty(t)$ for a very large radius, and the simultaneous difficulties of measuring very small velocities in a turbulent atmosphere coupled with superposition of other (nonsymmetric) vortex flow contributions make the extraction of $\Gamma_\infty(t)$ very difficult and inaccurate. Because the average circulation, defined by

$$\bar{\Gamma} \equiv \frac{1}{r_{\max}} \int_0^{r_{\max}} \Gamma(r)\, \mathrm{d}r \tag{5}$$

asymptotes toward Γ_∞ for large r (in an inviscid flow), average circulation levels are used to estimate Γ_∞.

On the other hand, circulation can be computed directly from the numerical simulations because vorticity can be integrated over an arbitrarily prescribed area to make the calculation without any ambiguity. By choosing a circular integration contour that is substantially larger than the vortex core, $\Gamma_\infty(t)$ can be estimated rather accurately. To compare experimentally measured circulation decay with calculated decay, it was decided that comparing the normalized (with respect to initial circulation) ratios of instantaneous circulation was preferred to matching the simulation output using the approximations required for the extraction techniques employed in the experimental measurements. Hence, we have used the computed instantaneous vorticity data in our simulations to locate the centers of the primary wake vortex cores, and the computed instantaneous circulation was normalized at a radius of 30 ft (9.1 m) about the located vortex center for the reference case. Subsequently, instantaneous circulation was normalized with respect to its initial maximum value.

Our two-dimensional, unsteady numerical simulations of the wake vortex flowfield were initiated at heights above the ground that corresponded to the actual aircraft flyby altitude for the particular flight test. That initial height assumption is in error because it implies that the aircraft wake rolls up immediately behind the generating aircraft[18]; however, that level of approximation is consistent with the accuracy of the current model. In addition, we have used asymptotic techniques to initialize the vortex flowfield, assuming that the atmosphere was quiescent and isothermal[19] to minimize numerical oscillations at the beginning of the simulations. The specific surface weather conditions were introduced in the simulation as a superimposed, uniform (horizontally) stratified crossflow where

the surface boundary layer velocity and temperature profiles were assumed to vary only with height (z). Hence, during a brief simulation time interval (approximately five dimensionless time units, which were defined as the initial circulation divided by the square of the initial vortex half-span), the superposition of the simplified initial vortex flowfield with the imposed, horizontally uniform weather produced a nonphysical flow relaxation transient. While the initial vortex flow was allowed to merge with the prescribed surface weather conditions, the atmospheric specifications were only imposed subsequently as inflow and outflow boundary conditions at the extreme limits of the numerical grid, which approximated infinite distances using the nonuniform grid system. To maintain the regions of very fine grid spacing in the vicinity of the vortex cores (in addition to the surface boundary region), it was necessary to convect the nonuniform grid horizontally using a constant crosswind velocity. Each simulation history required approximately 4 h of CPU time on the NAS Cray-90 machine and used 20 Mwords of memory. The numerical solutions were executed using dimensionless variables, and the only quantity that was influenced by changes in eddy viscosity was the equivalent Reynolds number. After the instantaneous vortex centers were located, the vorticity within $r = 9.1$ m was integrated numerically to obtain $\Gamma(t)$. It was then possible to compare $\Gamma(t)/\Gamma(0)$ with the dimensionless experimentally measured circulation histories for run 9. Three of the equivalent Reynolds number calibration tests, $R = \Gamma_\infty/\varepsilon = 3000$, $R = 800$, and $R = 300$, have been presented here as a basis for discussion. The normalized decay histories for upwind calibration vortices at the three equivalent Reynolds numbers, in an ambient environment that represented run 9 in the Idaho Falls test, along with the measured normalized decay history associated with the actual upwind vortex,[17] is shown in Fig. 3a. Similarly, the downwind vortices are compared with the experimental measurements in Fig. 3b.

The limitations of a constant eddy viscosity model are demonstrated in Fig. 3. It can be seen that the $R = 800$ approximation produces a very good representation of the measured decay for the upwind vortex, but underpredicts the decay rate for the downwind vortex. Furthermore, the nonphysical effect resulting from superposition of the initially symmetric vortex flow representation with a horizontally uniform initial surface weather approximation is apparent in Fig. 3, especially for $R = 3000$. The $R = 3000$ decay curve exhibits an increase in upwind circulation at the beginning of the simulation, resulting from the superposition of the initial wake vorticity with the crosswind vorticity. Because vorticity is associated with the crosswind velocity profile, the vortex circulation levels are increased for the upwind vortex and decreased for the downwind vortex during flow coupling for the first few dimensionless time units. That coupling transient is hidden for $R = 300$, because viscous decay occurs so rapidly that the circulation buildup for the upstream vortex cannot offset the decay. Because an aircraft in nonrolling flight produces equal but opposite sign circulation at both wing tips, regardless of the weather (assuming the pilot can respond perfectly to gusts, etc.), the superposition adjustment is inconsistent with the flow physics. Aside from that inconsistency, the $R = 800$ approximation was considered to be the best representation of the run 9 data because it produced the best representation of the stronger upwind vortex circulation history for the B 757 and was conservative in predicting the decay rate for the weaker downwind vortex circulation history.

Two methods were identified for eliminating the circulation inconsistencies resulting from the relaxation of the superimposed initial flows: 1) adjustment of the initial upstream and downstream circulation levels so that the relaxed upstream and downstream vortex circulations matched after the first few time units, or 2) neglect of the first few (initialization) time units, starting the circulation decay histories at the time that corresponded to the maximum circulation around the upstream vortex. The second approach was selected as the most realistic and practical approach. The logic for selecting that method was based upon the fact that the trial and error adjustment of the initial upstream and downstream vortex circulations produced a nonsymmetric initial flowfield that violated the assumptions that had been used to initialize the vortex flowfield. Furthermore, because viscous decay had also occurred during the relaxation time interval, the upstream and downstream vortices would not necessarily have matching circulation levels at that (arbitrary) time. Hence, the circulation decay histories used to examine the influences of surface weather conditions in this paper have been normalized in terms of the maximum circulation levels that were produced (either at the initial time for the downstream vortex or at the offset dimensionless time corresponding to the maximum circulation for the upwind vortex), rather than by assuming that the reference or maximum circulation levels occurred at $t = 0$.

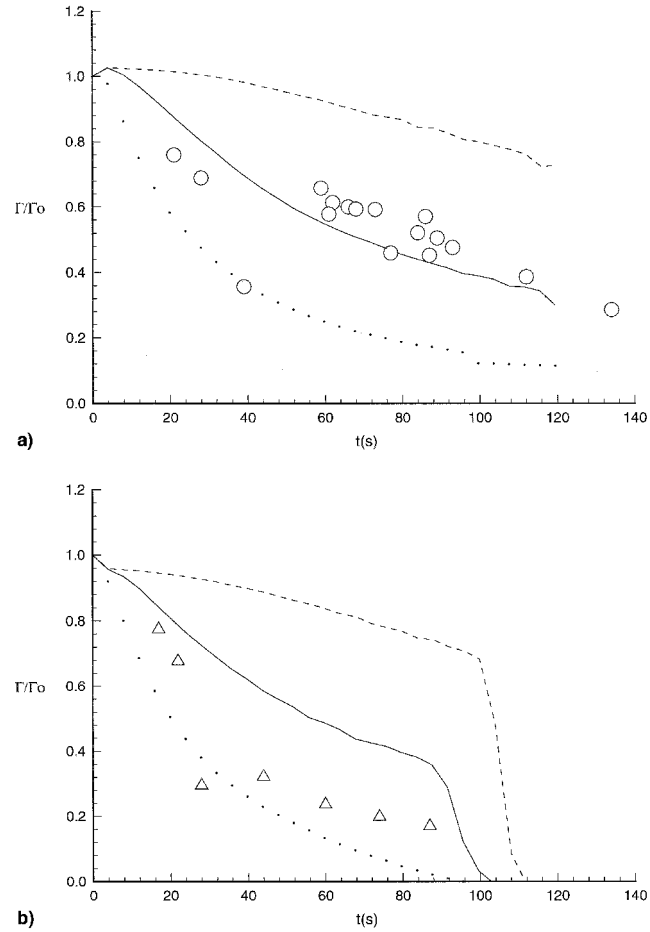

Fig. 3 Influence of equivalent Reynolds number on computed decay rate of wake vortices when subjected to run 9 weather conditions represented. ○, measured upwind vortex circulation; △, measured downwind circulation; ——, $R = 800$; – – –, $R = 3000$; ....., $R = 300$. Comparison of a) upwind and b) downwind vortices.

If $R = 800$ is taken as the equivalent Reynolds number for a B 757, the corresponding eddy viscosity ratio is given by $\varepsilon/\nu = 33{,}000$. Conversely, we could have proceeded by adopting a priori Squire's[12] assumption that eddy viscosity scales with circulation, which yields

$$\Gamma_\infty/\varepsilon = \text{const} \equiv S_q \tag{6}$$

and attempted to determine the universal constant S_q, which we have called Squire's constant. That was the approach used by Owen,[13] but he contended that the eddy viscosity should not scale simply with circulation, because it implied that the

Table 2 Comparison of S_q measurements for different experiments

Experimenter	Γ_∞/ν	S_q
Dosanjh et al.[23]	2×10^3	200
Newman[22]	2×10^4	500
Templin[21]	5×10^4	710
Mabey[20]	5×10^4	670
Run 9 (present test)	2.6×10^7	800

equivalent Reynolds number was the same for all aircraft. He developed a logical argument to support his contention that $\Gamma_\infty/\varepsilon$ scaled with the square root of Γ_∞/ν, and tested his model against most of the known experimental data available at that time.[20–24] However, Owen's comparisons[13] did not justify the more complex approximation, showing instead that there was scatter in S_q. To the contrary, if the flight experiments of Rose and Dee[24] are excluded from Owen's comparisons,[13] S_q values are consistent and can be tabulated. As shown in Table 2, S_q is nearly constant for circulation-based Reynolds numbers varying by three orders of magnitude. Those data suggest that the experiments of Dosanjh et al.[23] exhibit low Reynolds number effects.

Although not tabulated, higher values of S_q have been estimated from other experiments. The experimental measurements of Lezius[14] yield $S_q = 2000 \pm 500$, for $4 \times 10^4 < \Gamma_\infty/\nu < 2 \times 10^5$, while Owen[13] estimated that $S_q = 5000$ at $\Gamma_\infty/\nu \approx 10^7$ for the experiments of Rose and Dee.[24] Similarly, Iverson's[15] nonlinear eddy viscosity model was fit through a slightly different data set that produced $S_q \approx 10{,}000$ at $Re = \Gamma_\infty/\nu = 2.6 \times 10^7$. As previously noted, flight-test experiments are extremely difficult to control and to analyze. Furthermore, ground coupling causes significant departures from Squire's axisymmetric velocity distribution model.[12] While the Lezius[14] tow tank experiments were not flight experiments, the finite cross section of the tank likely altered the vortex trajectories and decay behavior, therefore affecting his estimates of eddy viscosity. The higher estimates for S_q appear to result from discrepancies between the model flow and the experiments rather than from Reynolds number influences.

Our numerical experiments do not support $S_p > 1000$ in modeling decay (see the $R = 3000$ plot in Fig. 3), and the simulations have also shown that actual wake vortex behavior in flight experiments is more complex than that predicted by a constant eddy viscosity model.[8] However, the assumption that Squire's constant[12] is only varying slowly and is approximately 800 over the Reynolds number range characterizing commercial flight appears to be consistent with the measurements of others and the limitations of the eddy viscosity model. Hence, $S_q = 800$ was used for all of our subsequent simulations.

Representative Aircraft/Weather Simulations

Using $R = 800$ for all six test cases, we investigated the ability of the constant eddy viscosity model to predict wake vortex motion and decay in comparison with the experimental measurements. The circulation decay histories for the three B 757 tests are shown in Fig. 4, and the circulation decay histories for the two B 767 cases and the B 727 case are shown in Figs. 5 and 6, respectively, along with the corresponding experimental data. Note that although the experimental data points are scattered, the simulations appear to be reasonably good in predicting the upwind decay histories and conservative in predicting the downwind circulation decay histories for all three aircraft types in all six weather states. The rapid decay at later times in many of the downwind vortices was partially because of a loss in numerical resolution as the downwind vortex convected rapidly out of the computational domain.

A two-dimensional simulation cannot accurately predict a three-dimensional flowfield. However, when the wake vortex generating aircraft is flying at constant altitude and speed, it is possible to assume a three-dimensional quasi-steady-state approximation where the third coordinate is generated perpendicular to the two-dimensional plane by multiplying the numerical time step by the aircraft speed. That approach has been used to develop three-dimensional vortex trajectory representations for the six flight tests. The horizontal paths followed by the upwind and downwind vortices are represented in Figs. 7–9 for the three different aircraft types. The x direction is

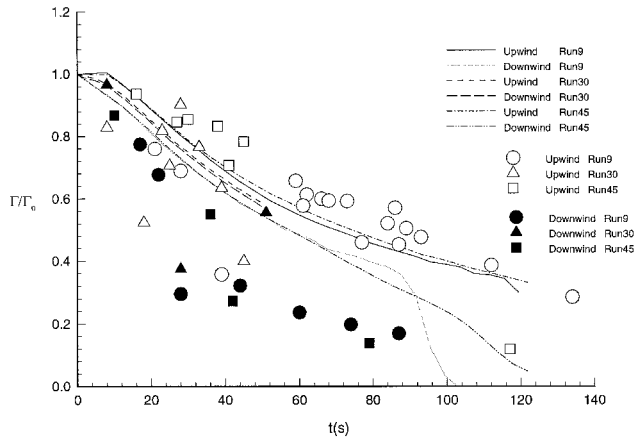

Fig. 4 Comparison between measured and simulated circulation decay histories for three B 757 tower flyby tests. See Table 1 and Figs. 1 and 2 for more details.

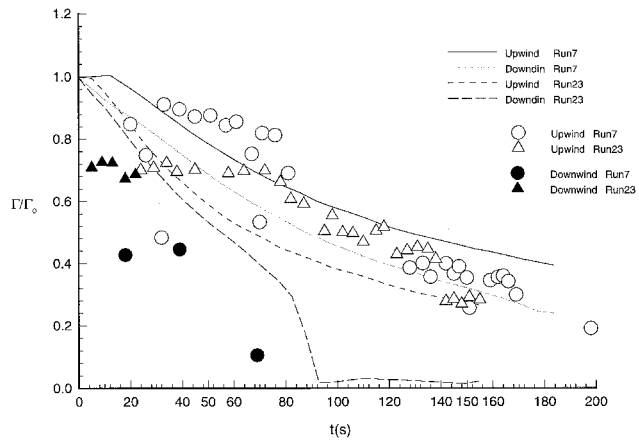

Fig. 5 Comparison between measured and simulated circulation decay histories for two B 767 tower flyby tests.

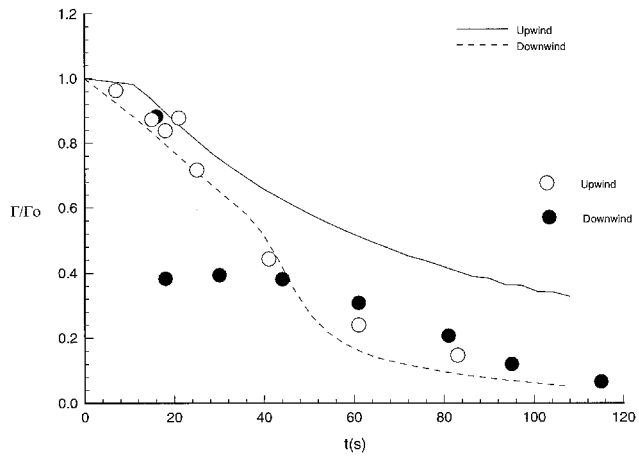

Fig. 6 Comparison between measured and simulated circulation decay histories for the B 727 tower flytest designated as run no. 22.

perpendicular to the aircraft line of flight (y direction), and $x = 0$ corresponds to the meteorological tower base. One B 757 flight test (run 30) was conducted with the wind blowing in the opposite direction to the other tests; thus, the aircraft flight path was on the opposite side of the tower and the vortex axes traversed from initial positive locations to negative positions.

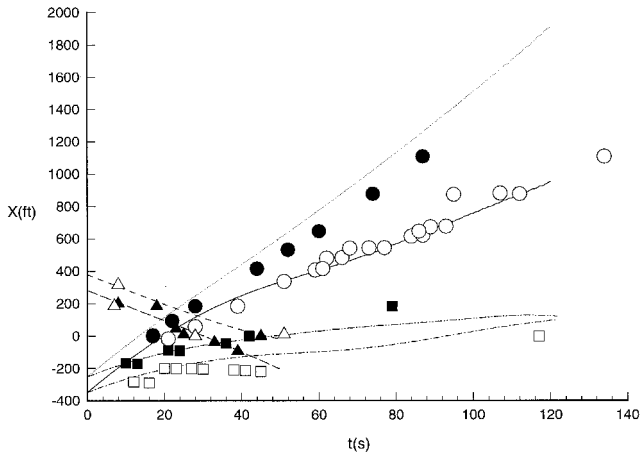

Fig. 7 Comparison between measured and simulated horizontal vortex (center) position histories for B 757 tower flyby tests (see Fig. 4 for legend).

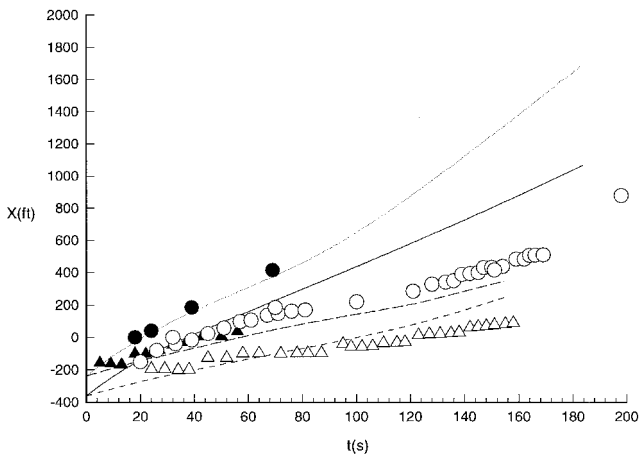

Fig. 8 Comparison between measured and simulated horizontal vortex (center) position histories for B 767 tower flyby tests (see Fig. 5 for legend).

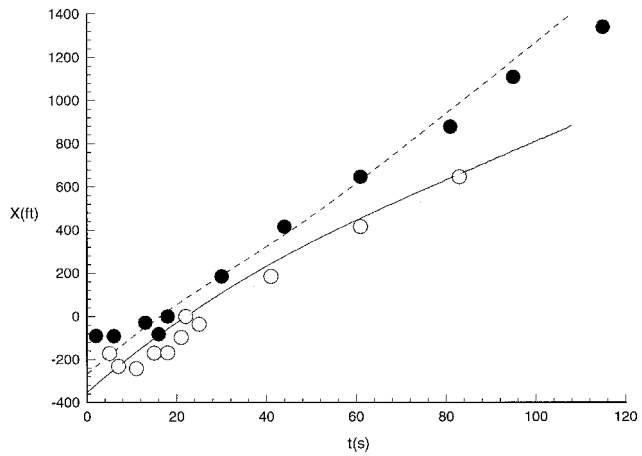

Fig. 9 Comparison between measured and simulated horizontal vortex (center) position histories for B 727 tower flyby test designated as run no. 22 (see Fig. 6 for legend).

The vertical position histories of the upwind and downwind vortices are shown in Figs. 10–12 for the three aircraft types. Those trajectories are remarkably varied and the simulations are in reasonable agreement with the measurements. Overall, we have concluded that $S_q = 800$ produces useful simulations of the flight-test data.

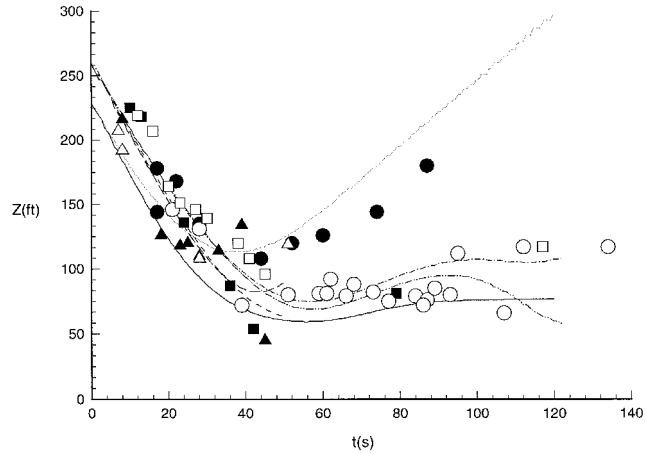

Fig. 10 Comparison between measured and simulated vertical vortex (center) position histories for B 757 tower flyby tests (see Fig. 4 for legend).

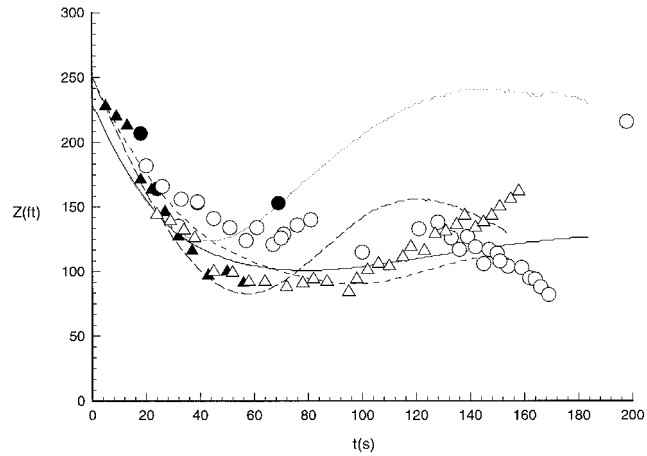

Fig. 11 Comparison between measured and simulated vertical vortex (center) position histories for B 767 tower flyby tests (see Fig. 5 for legend).

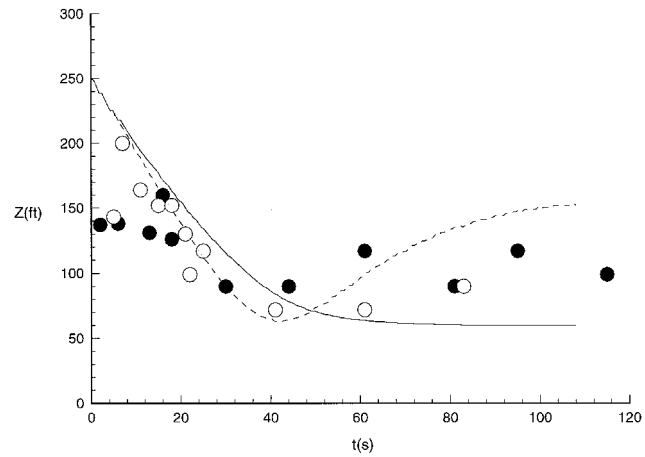

Fig. 12 Comparison between measured and simulated vertical vortex (center) position histories for B 727 tower flyby test designated as run no. 22 (see Fig. 6 for legend).

Table 3 Commerical aircraft characteristics

Aircraft type	Wing span, ft	Maximum landing weight, 1000 lbs	Landing speed, kn	s_o, m	Γ_∞, m^2/s	Γ_∞/s_o, m/s
B 737-200	93.0	103.0	129	11.13	253.0	22.73[a]
B 727-200	108.0	154.5	133	12.92	316.9	24.53[a]
B 757-200	124.5	210.0	137	14.90	362.8	24.35
A 310-200	144.0	271.2	139	17.24	278.8	16.17
B 767-200 ER	156.1	285.0	139	18.70	387.0	20.70
A 300-600	147.1	308.7	135	17.60	457.9	26.02[a]
DC 10-10	155.3	363.5	128	18.60	536.8	28.86
A 330	195.4	383.6	137	23.40	422.2	18.04
L1011-500	164.3	368.0	149	19.66	468.5	23.83[a]
DC 10-30	165.4	421.0	145	19.80	517.3	26.13[a]
B 777-200	199.9	445.0	138	23.90	465.2	19.88
MD 11	169.5	430.0	148	20.30	505.0	24.88[a]
B 747-400	211.0	630.0	153	25.30	575.0	22.73[a]

[a]Characteristic velocity is within 10% of B 757 value.

Generalized Wake Vortex Weather Effects

The numerical simulations that were used to produce the graphs in Figs. 4–12 were produced for $R = 800$, using dimensionless variables. Velocity was scaled by Γ_∞/s_o, where $2s_o$ is the initial vortex spacing and is related to the wing span b of the particular commercial aircraft. Similarly, length was scaled by s_o and time by s_o^2/Γ_∞. If s_o is assumed, given by[3]

$$s_o = \pi b/8$$

we can tabulate the velocity, length, and time scales for characteristic commercial aircraft using the database developed by Stuever.[25] The data shown in Table 3 represent a range of commercial aircraft types and can be considered to be representative of the commercial aircraft fleet.

To the accuracy of the $S_q = 800$ approximation, the data in Table 3 can be used to develop estimates of the influence of surface weather on wake vortex behavior for a variety of aircraft types. The universal aspects of the constant eddy viscosity model can only be used in terms of the dimensionless representations of the aircraft and surface weather data. For example, the magnitude of the measured crosswind is not influenced differently for the seven aircraft types indicated by asterisks in the table. However, the strain rate associated with the crosswind changes substantially between a B 727-200 and a B 747-400, because the initial vortex half-spacing varies by almost a factor of 2. Hence, if one refers to the weather conditions for the B 727-200 flight test utilized in this study (run 22 in Figs. 1 and 2), the weather conditions that are simulated for a B 747-400 would have essentially the same velocity magnitude, but the vertical variation would occur more slowly for the corresponding B 747-400 case (where the velocity and temperature that characterize the vertical location of 150 m in the figure would correspond to a vertical location of 290 m for B 747).

The circulation history, which was computed for an integration radius of 30 ft for the B 757 reference case (in dimensionless variables), corresponds to an integration radius of 26 ft for a B 727 circulation history and a radius of 51 ft for a B 747 circulation history. Because the circulation histories are normalized with respect to their maximum levels, these variations in integration radius are relatively unimportant. In addition, although these scalings alter the local variations of the Richardson number and Brünt–Väisällä frequency associated with the surface weather, influences as a result of those effects are rather small because of the strong coupling of the ground plane boundary.[8] Consequently, the weather cases that have been simulated for a B 757 at $S_q = 800$ are somewhat different than the corresponding weather for other aircraft types with different characteristic lengths and velocities. Furthermore, because the circulation decay times scale with s_o^2/Γ_∞, the circulation histories decay at somewhat different rates, depending on the aircraft characteristics. However, as long as a single aircraft type is being investigated, the surface weather and decay histories are all represented by the same scales, and the effects of weather on vortex behavior can be examined to the levels of the approximations used in this study.

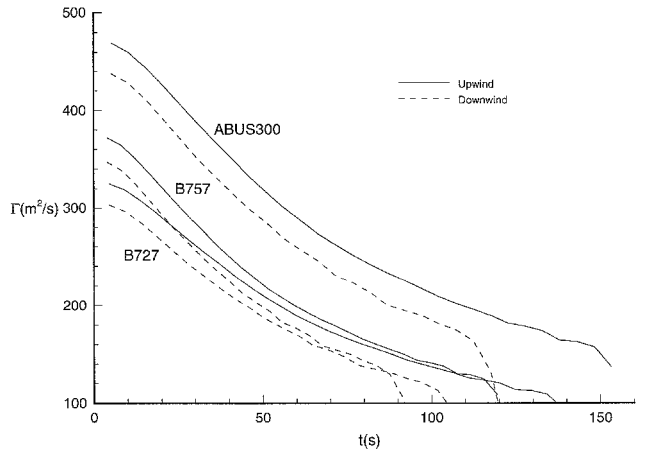

Fig. 13 Representations of circulation decay histories for three aircraft types subjected to surface weather conditions represented by run 9.

Generalized Circulation Decay Predictions

To the accuracy of the two-dimensional, constant eddy viscosity approximations, we can use our six flight test simulations to study how surface weather can influence wake vortex motion and circulation decay for different aircraft types. Using the simulation of run 9 as an example, we can examine the circulation decay histories for different aircraft types subjected to similar surface weather conditions. Here we mean similar in the sense that the surface wind profiles have the same variational magnitudes, but the vertical axis in the surface weather plot (of Fig. 1, for example) is true height only for one aircraft configuration (a B 757). The vertical axis of the weather data for other aircraft types represented by that simulation must be scaled for each aircraft type by the ratio of the particular value of s_o, from Table 3, to the actual reference value of s_o, i.e., 14.90 m, in the run 9 case for B 757. Hence, we can approximate the circulation decay behavior for B 727, B 757, and A 300, subjected to surface weather conditions that are similar to run 9 (Fig. 13). Here the influence of characteristic time is obvious, but the associated variations in surface weather conditions are more subtle.

Of greater interest is the question of how different surface weather states influence the wake vortex hazard conditions re-

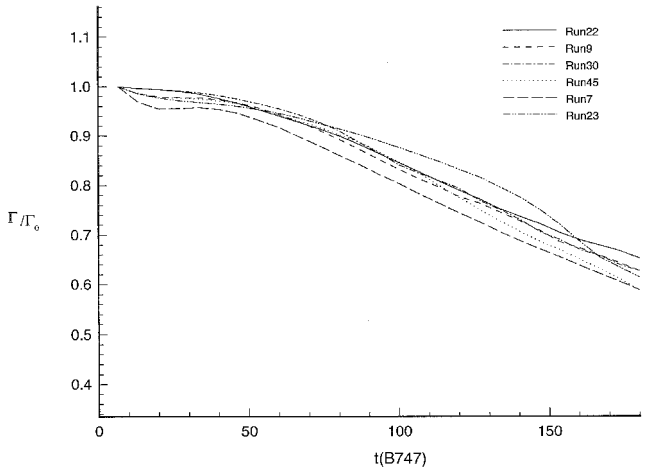

Fig. 14 Simulated upwind vortex circulation decay histories for B 747 wakes subjected to the surface weather conditions represented in Figs. 1 and 2 (see Table 1 for run number and meteorological data summaries).

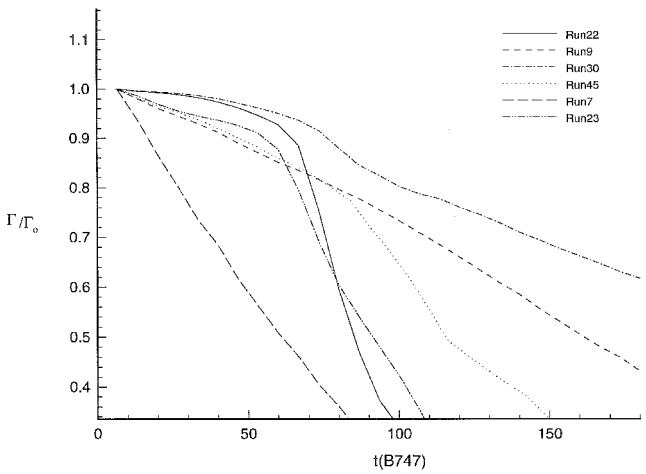

Fig. 15 Simulated downwind vortex circulation decay histories for B 747 wakes subjected to the surface weather conditions represented in Figs. 1 and 2.

sulting from a particular aircraft. Subject to the limitations resulting from our two-dimensional, constant eddy viscosity approximations, we can address that issue. Here we consider a hypothetical B 747-400, because it is one of the largest airplanes in the commercial fleet. The surface weather data presented in Figs. 1 and 2 can be used for a 747 representation if they are scaled by multiplying the vertical heights by 25.30 m/$s_{0_{ref}}$, where $s_{0_{ref}}$ is the characteristic wake vortex half-span for the particular aircraft represented by the simulation (B 757, 767, or 727). Because the circulation strength is higher for the upwind vortex than for the downwind vortex, we can compare the upwind circulation decay histories predicted for a 747 subjected to the six different surface weather states (Fig. 14). There each decay history is designated by the run number indicated in Table 1. The decay histories of the downwind vortices for a B 747 subjected to the six weather states are shown in Fig. 15. The influence of weather on the downwind vortex decay is more dramatic; however, much of the rapid decay effect (exhibited for runs 22 and 23) is because the vortex is convected out of the high-resolution portion of the computational domain rather than an actual physical effect.

Figure 14 shows that decay of the upwind vortex is nearly the same for the weather conditions represented by runs 9, 30, 45, and 22. However, during the first 2 min, the upwind vortex associated with run 23 remains much stronger than the other vortices, whereas the vortex associated with run 7 decays more rapidly than any other case over the entire time history. Because runs 7 and 23 are both associated with the same aircraft type (B 767), the differences cannot be attributed to scaling effects. Even more problematic is the fact that runs 7 and 9 can be characterized as almost identical weather states from a meteorological standpoint, and run 9 has a vortex decay history that can be called nominal with respect to the cases that were tested. However, a more careful examination of the weather conditions in Figs. 1 and 2 for run 9 as compared with run 7 reveals that run 7 has a nearly uniform crosswind shear and a much larger temperature variation away from the ground than does run 9. Run 9 also has virtually no wind shear away from the ground. Hence, even though the gross atmospheric features of the two runs can be described as stable with moderate shear, the details of the variations have exhibited significantly different influences on the rate at which the upwind vortex decays. These differences emphasize the utility of the constant eddy viscosity, two-dimensional simulation approach.

From the perspective of hazard forecasting, we can look at the *e*-folding time for each of the decay histories, observing that it takes the vortex associated with run 22 approximately 180 s to reach the 63.2% decay level, whereas the vortex associated with run 7 has decayed to that level in approximately 152 s. Using a B 747 landing speed of 153 kn, that difference in decay rate translates to a difference in spacing requirements of 1.2 n mile. More specifically, on days when the weather conditions are represented by run 7 (stable, with moderate shear and with nominally constant vertical temperature and velocity gradients), aircraft can be spaced more closely together without incurring any increase in hazard. Similarly, when the wind levels near the surface are nearly uniform (with almost no shear), as represented by the weather associated with run 23, the initial vortex decay rate is very slow, and increases in separation specifications are desirable when the crosswind causes either vortex to remain in the terminal flight corridor.

Finally, the actual airport layout must be considered before any of these results can be used. Because the rate at which aircraft wake vortices decay is only important during the time interval when one of the vortices is within or very near aircraft approach corridors, the actual locations of the runways must be considered. If a single runway is being used, then it is only necessary to consider upwind vortex behavior because the downwind vortex is convected away almost immediately. The downwind vortex, as well as the upwind vortex, must be considered for parallel runways.

Conclusions

Our simulations have shown that the two-dimensional constant eddy viscosity numerical model can be useful in assessing how different combinations of aircraft and surface weather conditions alter the wake vortex hazard conditions. Obviously, the constant eddy viscosity model cannot predict details of the wake vortex trajectory with great accuracy because of the inherently diffusive character of the approximation. However, gross motion and circulation decay can be predicted with accuracies that appear similar to those associated with other types of empirical correlations.

In addition, these simulations have shown how the natural dimensionless groups associated with length, time, and velocity can be used to scale flight-test data from one aircraft to another around airports. Near the ground, where buoyancy effects are damped strongly, shifts in Brünt–Väisällä frequencies associated with different aircraft exert only small changes in decay rate, even though vertical vortex position histories vary significantly. On the other hand, as demonstrated in the different decay rates between two very similar meteorological cases (runs 7 and 9), differences in shear and in temperature gradient in the upper portions of the surface zone can strongly influence wake vortex lifetimes.

Acknowledgments

This work was sponsored by NASA Langley Research Center under Grant NAGI-1437. Fred H. Proctor was the Grant Monitor. The authors would thank George C. Greene of NASA Langley Research Center for many helpful discussions and Dale V. Bloodgood for his assistance in preparing many of the graphs.

References

[1]"Airman's Information Manual," FAA, June 1995.

[2]Critchley, J. B., and Foot, P. B., "United Kingdom Civil Aviation Authority Wake Vortex Database: Analysis of Incidents Reported Between 1972 and 1990," *Proceedings of the FAA International Wake Vortex Symposium*, edited by J. N. Hallock, U.S. Dept. of Transportation, DOT/FAA/SD-92/1.1, Washington, DC, June 1992, pp. 8-1–8-17.

[3]Milne-Thomson, L. M., *Theoretical Aerodynamics*, Dover, New York, 1958.

[4]Rudis, R. P., Burnham, D. C., and Janota, P., "Wake Vortex Decay near the Ground Under Conditions of Strong Stratification and Wind Shear," *Proceedings of the AGARD Conference on the Characterization and Modification of Wakes from Lifting Vehicles in Fluids* (Trondheim, Norway), CP-584, AGARD, 1996, pp. 11-1–11-10.

[5]Donaldson, C. duP., and Bilanin, A. J., "Vortex Wakes of Conventional Aircraft," AGARDograph 204, May 1975.

[6]Hallock, J. N., *Proceedings of the FAA International Wake Vortex Symposium*, Vols. 1 and 2, U.S. Dept. of Transportation, Washington, DC, 1991.

[7]Zeman, O., "The Persistence of Trailing Vortices: A Modeling Study," *Physics of Fluids*, Vol. 7, No. 1, 1995, pp. 135–143.

[8]Zheng, Z. C., and Ash, R. L., "A Study of Aircraft Wake Vortex Behavior near the Ground," *AIAA Journal*, Vol. 34, No. 3, 1996, pp. 580–589.

[9]Zheng, Z. C., and Ash, R. L., "Prediction of Turbulent Wake Vortex Motion near the Ground," *Transitional and Turbulent Compressible Flows*, edited by L. D. Kral and T. A. Zang, Vol. 151, Fluids Engineering Div., American Society of Mechanical Engineers, New York, pp. 195–207.

[10]Landau, L. D., and Lifshitz, E. M., *Fluid Mechanics*, Pergamon, New York, 1966, Sec. 4.

[11]Bandyopadhyay, P. R., Stead, D. J., and Ash, R. L., "Organized Nature of a Turbulent Trailing Vortex," *AIAA Journal*, Vol. 29, No. 10, 1991, pp. 1627–1633.

[12]Squire, H. B., "The Growth of a Vortex in Turbulent Flow," *Aeronautical Quarterly*, Vol. 16, Aug. 1965, pp. 302–306.

[13]Owen, P. R., "The Decay of a Turbulent Trailing Vortex," *Aeronautical Quarterly*, Vol. 21, Feb. 1970, pp. 69–78.

[14]Lezius, D. K., "Water Tank Study of the Decay of Trailing Vortices," *AIAA Journal*, Vol. 12, No. 8, 1974, pp. 1065–1071.

[15]Iverson, J. D., "Correlation of Turbulent Vortex Decay Data," *Journal of Aircraft*, Vol. 13, No. 5, 1976, pp. 338–342.

[16]Garodz, L. J., and Clawson, K. L., "Vortex Wake Characteristics of B757-200 and B767-200 Aircraft Using the Tower Fly-By Technique," National Oceanic and Atmospheric Administration, TM Environmental Research Lab., Air Resources Lab. Rept. 199, Jan. 1993.

[17]Anon., "Atmospheric and Vortex Description for Idaho Falls B-757 Run 9 on September 25, 1990, Revision No. 1, April 1994," System Resources Corp., Burlington, MA, 1994.

[18]Huenecke, K., "Structure of a Transport Aircraft-Type Near Field Wake," *Proceedings of the AGARD Conference on the Characterization and Modification of Wakes from Lifting Vehicles in Fluids* (Trondheim, Norway), CP-584, AGARD, 1996, pp. 5-1–5-9.

[19]Zheng, Z., and Ash, R. L., "Viscous Effects on a Vortex Wake in Ground Effect," *Proceedings of the FAA International Wake Vortex Symposium*, edited by J. N. Hallock, U.S. Dept. of Transportation, DOT/FAA/SD-92/1.1, Washington, DC, 1992, pp. 31-1–31-30.

[20]Mabey, D. G., "The Formation and Decay of Vortices," DIC Thesis, Imperial College, London, 1953.

[21]Templin, R. J., "Flow Characteristics in a Plane Behind the Trailing Edge of a Low Aspect Ratio Wing as Measured by a Special Pressure Probe," National Aeronautical Establishment of Canada, Rept. LM AE-58, 1954.

[22]Newman, B. G., "Flow in a Viscous Trailing Vortex," *Aeronautical Quarterly*, Vol. 10, May 1959, pp. 149–162.

[23]Dosanjh, D. S., Gasparek, E. P., and Eskinazi, S., "Decay of a Viscous Trailing Vortex," *Aeronautical Quarterly*, Vol. 13, May 1962, pp. 167–188.

[24]Rose, R., and Dee, F. W., "Aircraft Vortex Wakes and Their Effects on Aircraft," Royal Aircraft Establishment, TN Aero 2934, Farnborough, England, UK, 1963.

[25]Stuever, R. A., "Airplane Database," NASA Langley Research Center, Hampton, VA, 1995.